

# Simulated holographic three-dimensional intensity shaping of evanescent wave fields

Laura C. Thomson,<sup>1,2</sup> Graeme Whyte,<sup>3</sup> Michael Mazilu,<sup>4</sup> and Johannes Courtial<sup>1</sup>

<sup>1</sup>*Department of Physics & Astronomy, University of Glasgow, Glasgow G12 8QQ, UK*

<sup>2</sup>*Thales, 1 Linthouse Road, Glasgow G51 4BZ, UK*

<sup>3</sup>*Department of Chemical Engineering, University of Cambridge, Cambridge CB2 3RA, UK*

<sup>4</sup>*School of Physics and Astronomy, University of St Andrews, St Andrews KY16 9SS, UK*

The size of bright structures in travelling-wave light fields is limited by diffraction. This in turn limits a number of technologies, for example optical trapping. One way to beat the diffraction limit is to use evanescent waves instead of travelling waves. Here we apply a holographic algorithm, direct search, to the shaping of complex evanescent-wave fields. We simulate 3D intensity shaping of evanescent-wave fields using this approach, and we investigate some of its limitations.

© 2008 Optical Society of America

OCIS codes: 090.1760, 170.4520, 350.4855

## 1. Introduction

Optical tweezers trap microscopic objects using the light field's intensity maxima or minima (depending on the objects' refractive index). The smallest possible size of high-visibility extrema, and the smallest possible separation between them, is given by the diffraction limit [1]. This in turn limits the resolution of optical trapping.

One way to overcome this resolution limit, that is to achieve superresolution, is to use superpositions of evanescent waves, whose transverse wavelength can be significantly shorter than that of travelling waves with the same optical frequency. Superpositions of small numbers of evanescent waves have previously been used to create structured evanescent-wave fields for optical trapping [2] and sorting [3]. Another method to create structured evanescent-wave fields, which is less closely related to the work described in this paper, consists of geometrically imaging an absorptive object (using travelling waves, so the image contains no superresolution structure) and then turning the intensity distribution of this image into the intensity distribution of an evanescent-wave field [4]. All of the work described above has been very successful and has had unexpected side benefits such as the ability to manipulate very large numbers of objects simultaneously [2].

Note that there are other types of superresolution that have been applied to optical trapping. The first type uses the fact that materials with a negative refractive index can in principle perform perfect imaging [5] – including restoration of evanescent waves –, and has already been demonstrated experimentally in a specialized optical-trapping setup [6]. The second type, travelling-wave superresolution holography, is based on the possibility of smaller detail in a light beam's darker region; this has recently been investigated theoretically [7]. The third type, manipulation of the polarization near the focus in order to sharpen it, has been used for the manipulation

of molecules [8].

Here we apply a holographic algorithm to the shaping of superpositions of arbitrarily many evanescent plane waves. We demonstrate numerically that this approach can be used to shape the intensity distribution of evanescent-wave superpositions in three dimensions (3D); we confirm that these superpositions can possess sub-wavelength structure in the transverse direction; and we encounter a constraint, which we relate to previous theoretical predictions. We believe our results are applicable to a number of fields, for example optical trapping using evanescent waves [2] and the excitation of specific surface plasmons in standard Kretschmann attenuated total reflection (ATR) geometry [9].

Note that there is much earlier work on photographic evanescent-wave holography, which is concerned with the recording and reconstruction of holograms of evanescent-wave fields using interference with a reference beam [10–12]. There is also recent work on digital holographic microscopy, which digitally records holograms that are interference patterns of travelling and evanescent waves and then reconstructs these in the computer, allowing the visualization of superresolution structure [13]. Here, we extend this work to the case of computer-generated holograms for evanescent waves.

This paper is organized as follows. In section 2 we discuss a possible setup for the production of evanescent plane waves and superpositions thereof. Section 3 outlines our application of the direct-search (DS) algorithm to 3D shaping of superpositions of such evanescent-plane-wave superpositions. Section 4 presents computer simulations that demonstrate 3D shaping of the intensity of evanescent-wave fields using this approach and discusses some limitations. We conclude in section 5.

## 2. Creation of superpositions of evanescent waves

Our application of the direct-search algorithm to evanescent-wave shaping (section 3) is written with a specific experimental design in mind (but it can be applied more generally). Here we outline two possible designs for the controlled creation of superpositions of evanescent plane waves.

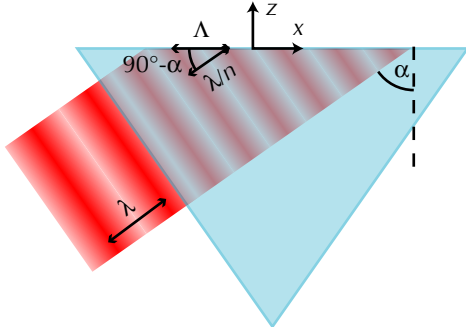


Fig. 1. (Color online) Geometry of the creation of evanescent waves by total internal reflection of a prism surface. A plane wave of vacuum wavelength  $\lambda$  is incident on a prism surface with angle of incidence  $\alpha$ . The transverse wavelength along the prism surface,  $\Lambda$ , is given by the equation  $\Lambda \sin(\alpha) = \lambda/n$ .

Fig. 1 shows the geometry of a plane wave entering a glass prism and hitting its top side, where total internal reflection (TIR) is taking place. The wavelength outside the prism (in air) is  $\lambda$ , that inside the prism glass of refractive index  $n$  is  $\lambda/n$ . We choose our coordinate system such that the TIR surface is in the  $z = 0$  plane and that the plane wave in the prism is travelling perpendicular to the  $y$  direction. Above the prism, the evanescent waves have the form of plane waves, namely

$$u(x, y, z) = \exp(i(k_x x + k_z z)), \quad (1)$$

where  $k_x^2 + k_z^2 = (2\pi/\lambda)^2$  (in our coordinate system  $k_y = 0$ ). However, in evanescent waves  $k_z$  is purely imaginary, and the wave therefore decays exponentially in the  $z$  direction.

The smallest transverse wavelength that can be achieved in evanescent waves using TIR as described above is  $\lambda/n$ , which corresponds to grazing incidence at the TIR surface. Small transverse structures can be achieved with small transverse wavelengths, which in turn can be realized using high- $n$  glass. One example of a suitable glass is Schott SF11, which has a refractive index of  $n > 1.7$  for a wide range of wavelengths, and which is relatively cheap as it is frequently used in femtosecond-laser correction.

A more versatile configuration consists of a glass hemisphere (Fig. 2), which can be illuminated from any direction ( $k_y \neq 0$ ). The hemisphere's flat side acts as the

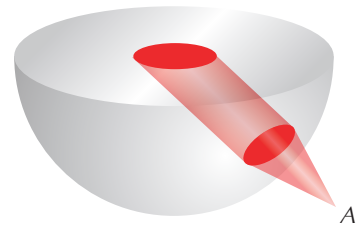


Fig. 2. (Color online) Glass hemisphere configuration creating an evanescent wave field in the centre of the flat surface. Illuminating the sphere with a point light source,  $A$ , which can be for example the end of a single-mode fiber, can create a collimated beam inside the glass, which in turn can create an evanescent plane wave above the centre of the hemisphere's flat side. Illuminating with two or more coherent point light sources at different positions can create a superposition of evanescent waves.

TIR surface. We propose to illuminate the hemisphere with a number of fiber ends, each effectively acting as a point light source. If a fiber end is positioned at the correct distance from the glass hemisphere, the curvature of the glass collimates the beam from the fiber inside the glass. The correct distance can be calculated from the lens maker's formula, which states that a spherical glass surface of refractive index  $n$  and radius of curvature  $r$  has a focal length

$$f = \frac{r}{n-1}. \quad (2)$$

Therefore each fiber end has to be positioned this distance  $f$  from the spherical surface to create a plane wave inside the glass hemisphere.

The different plane waves inside the glass hemisphere are then incident on the TIR surface, the hemisphere's flat side, from different directions, giving rise to different evanescent plane waves on the other side of the TIR surface. We limit ourselves to the case of all evanescent plane waves having the same global polarization, so they interfere.

The other ends of the illumination fibers are collected into a bundle and illuminated by a laser beam after it has interacted with a phase-only spatial light modulator (SLM). Specifically, the SLM is imaged onto the end of the fiber bundle, which means the phase at the positions of the input fiber ends – and therefore also at the output fiber ends – can be controlled directly. The intensity at the input fiber ends, and therefore also the intensity of the corresponding evanescent plane-wave components, is given by the intensity distribution of the illuminating laser beam.

## 3. Application of the direct-search (DS) algorithm to evanescent-wave shaping

With a view to potential applications in optical trapping, we aim to create superpositions of  $N$  evanescent plane-

wave components that have bright spots at  $M$  trap positions with coordinates  $(x_j, y_j, z_j)$  ( $j = 1, \dots, M$ ). We restrict ourselves to changing the phases of the evanescent plane waves, all of which are of the same intensity (generalization to different intensities is straightforward; a travelling-wave example can be found in Ref. [14]). We characterize the  $i$ th plane-wave component by its transverse wave-number values,  $k_{x,i}$  and  $k_{y,i}$ . The corresponding plane wave can then be written in the form

$$u_i(x, y, z) = \exp(i(k_{x,i}x + k_{y,i}y + k_{z,i}z)) \quad (3)$$

$$= \exp(i(k_{x,i}x + k_{y,i}y)) \exp(-\beta_i z), \quad (4)$$

where

$$k_{z,i} = \sqrt{(2\pi/\lambda)^2 - k_{x,i}^2 - k_{y,i}^2} \quad (5)$$

and  $\beta_i = -ik_{z,i}$  describes the exponential decay in the  $z$  direction. We then want to optimize the phases  $\phi_i$  of the plane-wave amplitudes in the superposition

$$v(x, y, z) = \sum_{i=1}^N \exp(i\phi_i) u_i(x, y, z) \quad (6)$$

such that the intensities at the trap positions  $(x_j, y_j, z_j)$ ,

$$I_j = |v(x_j, y_j, z_j)|^2, \quad (7)$$

are as bright and as equal as possible.

Direct search [14] is a brute-force approach to solving such “inverse” problems [15]. We apply it as follows. Initially, we set the phases of all beam amplitudes to random values. We then calculate the quality of the resulting superposition in terms of the intensity at the trap positions according to the definition

$$Q = \sum_j \ln(I_j + 1). \quad (8)$$

This definition is chosen to have two properties: 1) Increasing any one of the intensities  $I_j$  increases  $Q$ . 2) Transferring intensity from a brighter to a less bright trap position also increases  $Q$ . Now we make a random change to the superposition: we pick a random component and change the phase of its amplitude  $a_i$  to a random value. We calculate the quality of the altered superposition, again according to the definition (8), but calling this new quality  $Q'$ . If the new superposition is better than the old one, that is if  $Q' > Q$ , we accept the random change; otherwise we discard it. We repeat the process of randomly picking one component, randomly altering its phase, and keeping only changes that lead to improvements until the quality does not change any longer for several hundred iterations.

#### 4. Results

We have tested this approach to evanescent-wave shaping for various target distributions. Our results demonstrate

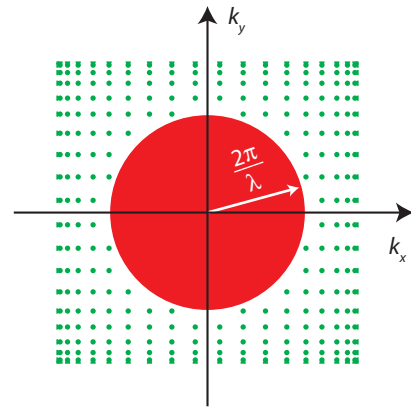


Fig. 3. (Color online) Example of the transverse wave numbers  $k$ -space distribution of evanescent plane-wave components used in our simulation. The dots represent evanescent-plane-wave components. They all lie outside the shaded area in the centre, which represents travelling waves.

that our approach works, but they also demonstrate its limits.

The simulations in this section were performed for specific choices of additional parameters. All our simulations were performed for  $\lambda = 632.8\text{nm}$ . We also made a choice on the specific arrangement of optical fibers around the glass sphere: our model represents an arrangement of optical fibers that are equally spaced in their projection angles into the  $xz$  and  $yz$  planes, whereby travelling-wave components are not allowed. An example of the corresponding  $k$ -space distribution is shown in Fig. 3.

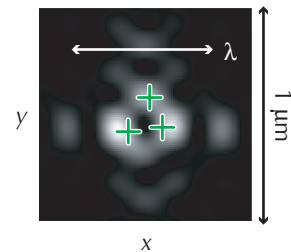


Fig. 4. (Color online) Shaping of the transverse intensity distribution of an evanescent-wave superposition, here directly above the prism surface ( $z = 0$ ). “+” symbols indicate positions where the intensity was maximized. The  $k$ -space components are those shown in Fig. 3.

Figure 4 demonstrates shaping of the transverse intensity distribution of the evanescent-wave field immediately above the hemisphere’s surface ( $z = 0$ ). It also demonstrates that the intensity features can be sub-wavelength in size.

The algorithm can also shape the transverse intensity in planes a finite distance above the hemisphere’s surface.

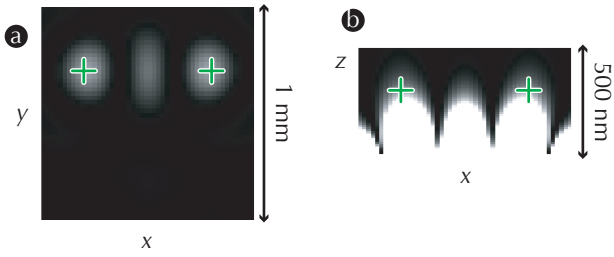


Fig. 5. (Color online) Transverse (a) and longitudinal (b) intensity cross-section after optimization of the intensity at two trap positions (“+” signs). The trap positions are 300nm above the prism surface. The  $k$ -space distribution is that shown in Fig. 3.

Fig. 5 shows the result of optimization of the intensity at two points a finite distance above the prism surface. Fig. 5(a) shows the transverse ( $x, y$ ) intensity cross-section away from the prism surface. The corresponding ( $x, z$ ) cross-section (Fig. 5(b)) demonstrates that, unlike in similar algorithms used for shaping travelling waves, simply optimising the intensity at a number of points does not produce 3D intensity maxima.

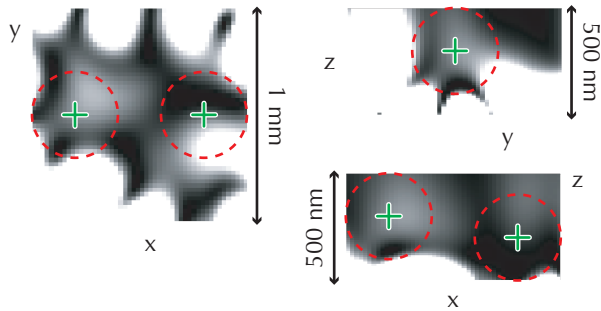


Fig. 6. (Color online) Intensity resulting from an attempt to force the creation of two 3D intensity maxima. The algorithm tries to maximize the intensity at the trap positions, which are indicated by “+” signs (green in the online version); it tries to minimize the intensity at the points marked with “-” signs (red in the online version).  $k$ -space distribution as in Fig. 3.

Figure 6 shows the results of attempting to force the creation of 3D intensity maxima. In addition to trap positions where the intensity is maximised, we modified the algorithm to minimise the intensity on a set of points on spheres around the maximum-intensity trap positions, simply by extending the definition of  $Q$  to include a term such that an increase of the intensity at any one of  $L$  “no-trap” positions  $(x_j, y_j, z_j)$ , where  $j = M + 1 \dots M + L$ , leads to a *decrease* of the quality:

$$Q = \sum_{j=1}^M \ln(I_j + 1) - \sum_{j=M+1}^{M+L} \ln(I_j + 1). \quad (9)$$

Interestingly, we did not succeed in creating 3D intensity maxima. This might well be due to the fact that we restrict ourselves to superpositions of evanescent plane waves that all have the same intensity. However, it might also be – fully or in part – due to a more fundamental reason related to Earnshaw’s theorem, as outlined in the following.

Earnshaw’s theorem states that it is impossible to have a field maximum or minimum in a volume of empty space for static electromagnetic fields. The theorem does not apply as such for electromagnetic waves, which indeed can be focussed in empty space. This is due to the wave nature of light and its interference properties. When considering sub-wavelength 3D focussing, as we do here, the volume of empty space where the maximum intensity is to be achieved is much smaller than the wavelength of the light. At this size scale the wave nature of light disappears and Earnshaw’s theorem becomes more and more applicable as the focussing volume is decreased [16, 17]. A more careful analysis [16, 17] translates this into a decreased efficiency when focussing smaller and smaller spots. This, in turn, is equivalent to low visibility of the shaped spots, which lie in a relatively dark area surrounded by a relatively bright area, as is typical for optical super-resolution [7].

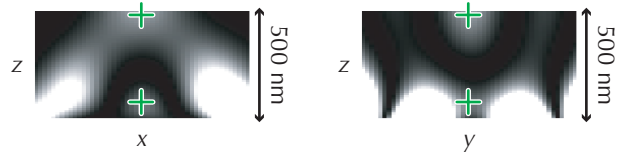


Fig. 7. (Color online) Demonstration of intensity maxima away from the prism interface. The intensity was maximized in two points, each marked with a “+”, on the line  $x = y = 0$ . The intensity is shown in two planes that both include the line:  $y = 0$  (a), and  $x = 0$  (b). What appears to be a 3D maximum in (a) turns out to be a saddle point in (b). The intensity was calculated for a  $k$ -space distribution different from that shown in Fig. 3.

Finally, we address the commonly held belief that the intensity of evanescent-wave fields can only ever fall off in the longitudinal direction. Fig. 7 demonstrates that, along a line in the transverse ( $z$ ) direction, the intensity can not only rise in the  $z$  direction, but it can also go through one or more maxima. (Note, however, that in 3D all of the intensity maxima along the line in the  $z$  direction are saddle points.) Fig. 8 explains how an out-of-phase superposition of exponential functions (such as amplitudes of different evanescent waves) can have a maximum; superpositions of more exponentials can have more maxima.

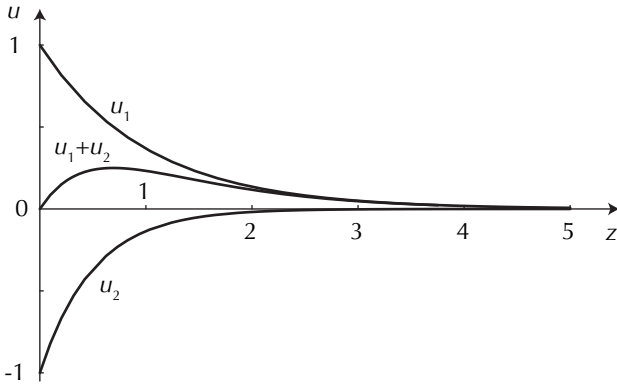


Fig. 8. Local maximum in the field,  $u$ , sum of two evanescent waves,  $u_1(z) = \exp(-z)$  and  $u_2(z) = -\exp(-2z)$  where  $z$  is the propagation distance (dimensionless units).

## 5. Conclusions and future work

In this work, we have investigated the potential use of evanescent-wave holography for optical micromanipulation. Our results are useful not only for showing that evanescent-wave intensities can be shaped in 3D, but also for investigating the limitations of holographic evanescent-wave shaping.

There are many ways in which our work can be extended. Firstly, for applications in optical trapping it would be useful to calculate stiffness, resolution, and efficiency (suitably defined) that can be achieved with evanescent-wave traps.

Secondly, the direct-search algorithm could be applied in many slightly different ways, and the different applications could be compared and contrasted. For example, the algorithm could optimize the phases in a mixture of evanescent and travelling waves, and it could be extended to take into account polarization. It is also possible to use a different algorithm altogether. The direct-search algorithm could, for example, be extended to become a simulated-annealing algorithm (see Ref. [18] for an explanation and comparison of different algorithms applied to travelling-wave intensity shaping), which is better at finding the global maximum of the quality function (direct search often only finds a local maximum).

Thirdly, other configurations or input constraints can be investigated such as allowing the intensity of the evanescent-plane-wave components to change. Our configuration is restricted to producing evanescent waves with transverse wavelengths  $\geq \lambda/n$ . A way to create evanescent-wave components with transverse wavelengths smaller than  $\lambda/n$  is the use of structured surfaces, in the simplest case a grating. Such a structure could be put on top of the prism/hemisphere, or it could simply be used on its own. (If the structure is placed on top of the prism, zero-order reflections are cut out). However, each travelling plane wave illuminating such a structure

produces not a single evanescent plane wave, but a superposition of evanescent plane waves. This clearly represents a slight complication, but one that could be taken into account in the algorithm.

## Acknowledgments

Thanks to Miles Padgett for useful discussions. LCT is supported by a CASE studentship. JC acknowledges generous support from the Royal Society (London) in the form of a University Research Fellowship.

## References

1. The size and separation of extrema can be arbitrarily small, provided their visibility is also arbitrarily small [19].
2. P. J. Reece, V. Garcés-Chávez, and K. Dholakia, “Near-field optical micromanipulation with cavity enhanced evanescent waves,” *Appl. Phys. Lett.* **88**, 221116 (2006).
3. T. Čížmár, M. Šiler, M. Šerý, P. Zemánek, V. Garcés-Chávez, and K. Dholakia, “Optical sorting and detection of sub-micron objects in a motional standing wave,” *Phys. Rev. B* **74**, 035105 (2006).
4. V. Garcés-Chávez, K. Dholakia, and G. C. Spalding, “Extended-area optically induced organization of microparticles on a surface,” *Appl. Phys. Lett.* **86**, 031106 (2005).
5. J. B. Pendry, “Negative refraction makes a perfect lens,” *Phys. Rev. Lett.* **85**, 3966–3969 (2000).
6. Z. Lu, J. A. Murakowski, C. A. Schuetz, S. Shi, G. J. Schneider, J. P. Samluk, and D. W. Prather, “Perfect lens makes a perfect trap,” *Opt. Express* **14**, 2228–2235 (2006).
7. L. C. Thomson, Y. Boissel, G. Whyte, E. Yao, and J. Courtial, “Simulation of superresolution holography for optical tweezers,” *New J. Phys.* **10**, 023015 (2008).
8. L. Helseth, “Smallest focal hole,” *Opt. Commun.* **257**, 1–8 (2006).
9. R. F. Wallis and G. I. Stegeman, eds., *Electromagnetic Surface Excitations* (Springer-Verlag, Berlin, 1986).
10. O. Bryngdahl, “Holography with evanescent waves,” *J. Opt. Soc. Am.* **59**, 1645–1650 (1969).
11. S. I. Bozhevolnyi and B. Vohnsen, “Near-field optical holography,” *Phys. Rev. Lett.* **77**, 3351–3354 (1996).
12. P. S. Ramanujam, “Evanescent polarization holographic recording of sub-200-nm gratings in an azobenzene polyester,” *Opt. Lett.* **28**, 2375–2377 (2003).
13. P. Marquet, B. Rappaz, P. J. Magistretti, E. Cuche, Y. Emery, T. Colomb, and C. Depeursinge, “Digital holographic microscopy: a noninvasive contrastimaging technique allowing quantitative visu-

- alization of living cells with subwavelength axial accuracy,” *Opt. Lett.* **30**, 468–470 (2005).
14. M. A. Seldowitz, J. P. Allebach, and D. W. Sweeney, “Synthesis of digital holograms by direct binary search,” *Appl. Opt.* **26**, 2788–2798 (1987).
  15. A. Tarantola, *Inverse Problem Theory* (SIAM (Society for Industrial and Applied Mathematics), Philadelphia, 2005).
  16. M. Mazilu and K. Dholakia, “Subwavelength trapping volumes created using negative refraction,” presented at SPIE Optics & Photonics 2006, San Diego, Calif., August 13 - 17, 2006.
  17. M. Mazilu and K. Dholakia, “Limits and possibilities in subwavelength imaging using negative refraction,” presented at Photon06, Manchester, UK, September 4 - 7, 2006.
  18. M. Clark and R. Smith, “A direct-search method for the computer design of holograms,” *Opt. Commun.* **124**, 150–164 (1996).
  19. M. Berry, “Faster than Fourier,” in “Fundamental Problems in Quantum Theory,” J. A. Anandan and J. Safko, eds. (World Scientific, Singapore, 1994).